Chemical Communication ChemComm

Cite this: DOI: 10.1039/c0xx00000x

www.rsc.org/xxxxxx

ARTICLE TYPE

Efficient cycloaddition of epoxides and carbon dioxide over novel organic-inorganic hybrid zeolite catalysts

Chen-Geng Li, Le Xu, Peng Wu*, Haihong Wu and Mingyuan He*

Received (in XXX, XXX) Xth XXXXXXXXX 20XX, Accepted Xth XXXXXXXXX 20XX

DOI: 10.1039/b000000x

Organic-inorganic hybrid zeolites with the MFI-type lamellar structure serve as efficient solid Lewis base catalysts for solvent-free synthesis of a variety of cyclic carbonates from corresponding epoxides and carbon dioxide. The ion-exchange with iodide, in particular, renders these materials an excellent catalytic activity and good recyclability

Organic structure-directing agents (SDA) are widely used in the synthesis of microporous zeolites, directing the formation of various crystalline frameworks with unique porosities. Zeolites usually suffer difficulties in catalyzing reactions involving bulky molecules. Such reactions cause severe diffusion problems when taking place inside micropores, limiting the application of zeolites.[1-3] One of alternative approaches to solve this problem is to design new SDAs that are capable of leading to new zeolite structures containing nanometer-scaled mesopores if possible.[4-6]

Despite high manufacturing costs, SDAs are always eliminated by calcination after completion of crystallization, rendering the zeolite pores open and to have a large surface area. The calcination may force the framework of zeolite precursors to destruct in some cases.[7-8] Davis et al. first proposed a protocol for reusing the SDA molecules occluded in as-synthesized ZSM-5 zeolites though unique processes of degradation and reassembling of SDA.[9] In this way, the calcination is avoided and the fragile zeolite structures might be well preserved.

Rather than extracting the SDAs out of zeolites, it is more economically saving and environmentally friendly if SDAs can be used directly as active sites for catalyses. Little attentions have been paid on utilizing the SDAs directly.[10] To serve as useful catalysts, the SDA-containing zeolite composite materials should satisfy the preconditions that these organic species are stable against leaching in organic solution and rigid enough against degradation under severe reaction conditions of high temperature and pressure. It is also important that theseactive sites located inside zeolite pores should be reachable by guest molecules. Recently, Ryoo et al. developed a series of Gemini-type surfactants that could lead to mesoporous MFI zeolites composed of ordered microporous nanosheets.[11] With one quaternary ammonium inside 10-membered ring (MR) channels of MFI zeolite sheets, the long alkyl groups and branch groups of SDA are then firmly immobilized against leaching. The other ammonium cations located in interlayer mesostructured spaces is thus accessible from outside. In fact, we demonstrated that the organic-inorganic lamellar ZSM-5 composite exhibited bifunctionalities as solid acid-base catalysts.[12]

The cycloaddition of carbon dioxide and epoxides is an important reaction for synthesizing value added cyclic carbonates, widely used in polymer industry, pharmaceutical and biomedical fine chemical synthesis,[18] and it is expected as an effective way for reducing carbon dioxide emission as well.[13] The activation of C=O bond is an essential issue in utilizing carbon dioxide via cycloaddition. By properly designing the catalysts such as metallic complexes[19-21], phosphines[22, 23], organic bases[24], ionic liquids[25, 26], metal oxides[27-29], mild conditions have been optimized for this reaction. Here, we communicate that an organic SDA embedded layered MFI zeolite cooperated synergistically with the post incorporated halogen anions in the cycloaddition reactions (Scheme 1), producing carbonates actively and selectively in a heterogeneous way.

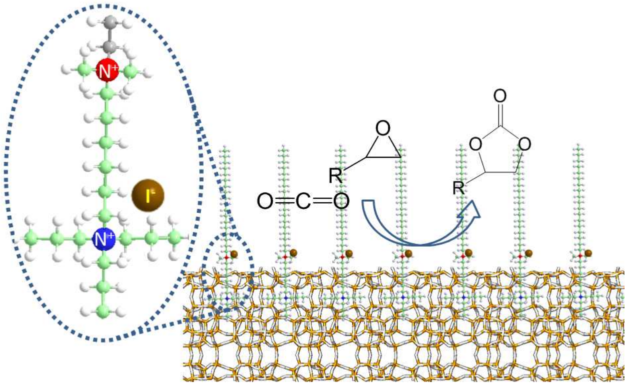

Scheme 1 Cycloaddition of epoxide and CO_2 over halogen anion-exchanged organic-inorganic hybrid zeolite catalyst.

The XRD patterns of lamellar MFI zeolite (LMFI-AS) as-synthesized with $[C_{18}H_{37}Me_2N^+(CH_2)_6N^+Pr_3]Br_2^-$ ($C_{18\text{-}6\text{-}3}$) showed a typical layered structure that was different from conventional three-dimensional MFI (Fig. 1 and ESI, Fig. S1). An oriented crystal growth made missing the corresponding reflections related to *b*-axis. The lamellar material was also featured by a diffraction in the low-angle region (2θ = 1.4°), which was attributed to the mesostructure consisting of zeolite nanosheets and occluded organic micelle layers. The SEM image showed that the morphology of LMFI-AS was of flower-like spheres composed of primary palette crystals (Fig. 1a). The high resolution TEM image further confirmed the presence of a uniform two-dimensional lamellar structure with the quaternary ammonium head groups buried within zeolite channels while the long alkyl chain groups pillaring the sheets. A repeated acid treatment with 1 M HI/EtOH solution made the mesostructure almost intact, as the XRD refection at small angle remained at the same position (ESI, Figure S1c), and well-preserved lamellar structure was still visible in TEM image (Fig. 1a and b). The anchoring of the diammonium groups inside zeolite channels firmly stuck the SDA from leaching by acid washing. Thus, the organic-inorganic hybrid zeolites were relatively stable in chemical composition, which rendered them possible applications as catalysts.

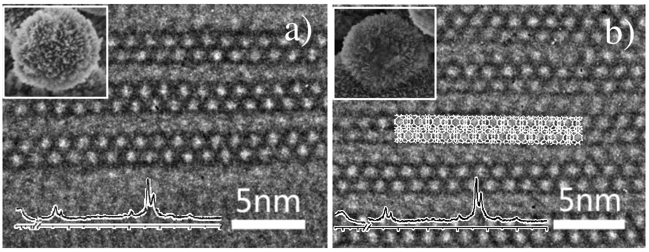

Fig. 1 SEM and HRTEM images as well as XRD patterns of LMFI-AS (a) and LMFI-HI (b) materials.

The quantity of organic species was measured by thermal gravimetric analysis (ESI, Fig. S2). The massive loss before 100 ºC corresponded to water physically adsorbed on the material and that over 500 ºC was because of the condensation of silanol groups. The materials showed the DTG peaks in the region of 200 - 500 ºC, which belonged to the SDA species inside channels. Those physically adsorbed on the external surface was decomposed in a lower temperature range of 200 - 250 ºC. The weight loss of LMFI-AS was 28.1%. The acid treatment effectively swept the SDAs physisorbed or loosely occluded on the external surface, resulting in a weight loss of 14.4% for LMFI-I. These remaining SDA organic species are presumed to be stuck firmly inside zeolite channels. The stability of $C_{18\text{-}6\text{-}3}$ containing propyl groups was confirmed by a multi-step acid treatment in comparison to $[C_{22}H_{45}Me_2N^+(CH_2)_6N^+Me_3]Br_2^-$ ($C_{22\text{-}6\text{-}3}$) which was less stable against acid washing (ESI, Fig. S3).

The compositions of C, H, N and I of lamellar zeolites were quantified by elemental analysis or ion chromatography (ESI, Table S1). The C/N ratios were slightly higher than the theoretical value of $C_{18\text{-}6\text{-}3}$ compound, probably as a result of a partial coke formation in hydrothermal synthesis. The difference in elemental composition before and after acid treatment was mainly due to the loss of those surfactant species that did not serve as SDA, but simply physisorbed on the crystal surface. The acid treatment easily swept this part of SDAs off the zeolite crystals. Nevertheless, by employing a bulky Gemini-type diquaternary ammonium surfactant containing propyl groups, stable hybrid composites were obtained even after acid washing.

The N_2 adsorption isotherms showed the acid treatment changed the adsorption capacity of lamellar MFI zeolite (Fig. 2).

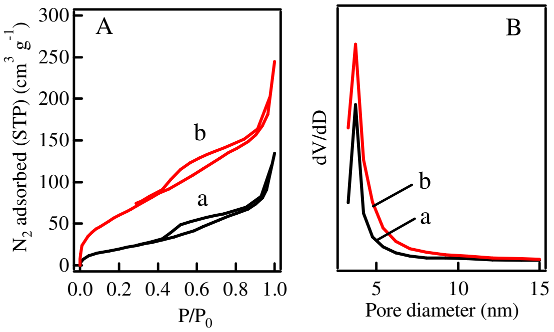

Fig. 2 N_2 adsorption/desorption isotherms (A) and pore diameter distribution (B) of LMFI-AS (a) and LMFI-I (b).

The LMFI-AS material adsorbed limited amount of nitrogen molecules and exhibited almost no micropore distribution, because the SDA molecules filled up both intralyaer micropores and most of interlayer mesopores. After extracting those removable SDA species, a part of mesopores became open, and the specific surface area increased from 80 m^2 g^{-1} for LMFI-AS to 239 m^2 g^{-1} for LMFI-I (ESI, Table S1), making interlayer spaces more accessible to guest molecules. However, the adsorption capacity of micropores did not change so much. This could also be a proof that the SDAs were firmly embedded inside zeolite channels not removable by acid washing. Both LMFI-As and LMFI-I showed a narrow mesopore distribution at 3.7 nm, which was approximately the length of alkyl tail in SDA. It is noteworthy that the interlayer distance was not a fixed value due to the flexibility of linear organic SDA.

Table 1 Cycloaddition of different epoxides with CO_2 over LMFI-I[a]

Entry	Substrate	Product	Conv. (%)	Sel. (%)	TON
1	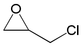	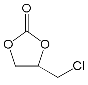	90.1	95.0	589
2	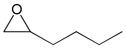	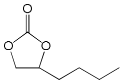	73.8	96.0	483
3	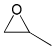	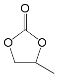	99.5	97.6	652
4	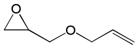	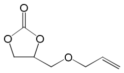	99.4	95.7	650
5	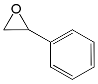	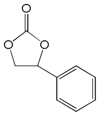	29.5	100	193

[a] Reaction conditions: LMFI-I 100 mg; substrate amount, 10 mmol; CO_2 pressure, 2.0 MPa; temp., 413 K; time, 4 h; no solvent.

Table 1 shows the catalytic performance of lamellar MFI zeolites in the cycloaddition of carbon dioxide and different epoxides under solvent-free conditions. No carbonate products were obtained when the reactions were carried out in the absence of catalyst for all the epoxides investigated at 413 K and 2.0 MPa CO_2 pressure for 4 hours, indicating non-catalytic activation of carbon dioxide was extremely difficult even under severe conditions. With the aid of LMFI-I catalyst, the epoxides were converted significantly, most of which showed a conversion over 90% and a carbonate selectivity over 95%. The byproducts were only diols formed from ring-opening of epoxides. The high carbonate selectivity suggested that the pairs of quaternary ammonium cations and halide anions were efficient catalytic active sites for cycloaddition. Styrene oxide showed a lower conversion likely because its bulky molecular size proposed a steric hindrance when approaching to the active sites. Since the interlayer mesopores were partly blocked by the alkyl tail of SDA, the diffusion limitation then retarded the reaction to a great extent. The specific catalytic activity or turnover number (TON) was calculated by referring the amount of converted ECH to that of I^- active sites used. LMFI-I gave a TON in the range of 193 – 652, indicating a high catalytic efficiency.

Herein, we employed epichlorohydrin (ECH) as the substrate to systematically investigate the catalytic properties of LMFI catalysts in the cycloaddition reaction. Table 2 compares the performance among various catalysts. Without the presence of catalyst, the expoxide was slightly consumed, and it was predominately hydrolysed to corresponding diol (No. 1). The S-1-I catalyst, prepared from conventional silicalite-1 as-synthesized with TPAOH and HI/EtOH washing, showed a ECH conversion of 44.6% and a carbonate selectivity of 73.6% (No. 2). The relatively high selectivity toward carbonate on S-1-I also demonstrated that the iodide effectively catalysed the reaction. However, its performance was obviously inferior to that of LMFI materials (Nos. 3 – 6). Possessing a three-dimensional MFI topology, the S-1-I material containing the TPA species inside channels possessed a low surface area of 80 m^2 g^{-1}. The cycloaddition took place only on TPA^+I^- located on the pore entrance and external surface of zeolite crystals. As the conversion of epoxide to carbonate was low, the possibility of hydrolysis of epoxide molecules diols became obvious, which lowered the carbonate selectivity. Thus, the lamellar zeolite composites had the advantages by containing simultaneously mesopores and quaternary ammonium species.

Among the LMFI materials ion-exchanged with various halogen anions (I^-, Cl^- and Br^-), the iodides proved to be the most efficient catalytic sites (Table 2, No. 4). The higher activity of iodides is attributed to its larger anion radius which weakens the bound of the valence electron with the nucleus. As a result, iodide is easier to attack the α-C on epoxides as in the first step of the catalytic circulation in comparison to chloride or bromide (ESI, Scheme S1). After the organic SDA species were eliminated completely by calcination, the LMFI-I-cal catalyst showed no activity to carbonate formation even though it had the highest surface area (No. 7). $C_{18-6-3}I_2$ as a homogeneous catalyst was also highly active to the reaction (No. 8), verifying the organic ammonium iodide in LMFI-I was the react active sites.

Table 2 Cycloaddition of carbon dioxide to ECH over different catalysts[a]

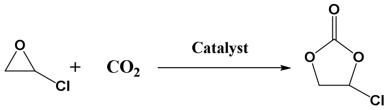

No.	Cat.	Conv. (%)	Sel. (%)	X content[b] (%)	S_{BET}[c] (m^2 g^{-1})
1	no cat	18.2	0	0	-
2	S-1-I	44.6	73.6	-[d]	2
3	LMFI-AS	62.7	88.8	-[d]	80
4	LMFI-I	90.0	95.0	1.94	239
5	LMFI-Cl	49.4	87.0	1.92	118
6	LMFI-Br	71.0	88.1	0.49	214
7	LMFI-I-cal	37.0	0	-[d]	837
8	$C_{18-6-3}I_2$[e]	99.4	97.0	-	-

[a] Reaction condition: cat., 100 mg; ECH, 10 mmol; CO_2 pressure, 2.0 MPa; temp., 423 K; time, 4 h; no solvent. [b] X = Cl, Br or I, quantified by ion chromatography. [c] Measured by N_2 adsorption at 77 K. [d] Not determined. [e] 10 mg of $C_{18-6-3}I_2$ used, with the same iodide content in 100 mg LMFI-I.

The influence of temperature on the cycloaddition of ECH and CO_2 over LMFI-I was investigated (ESI, Fig. S4A). The ECH conversion increased progressively with temperature and reached over 90% at 413 K. The activation of C=O in CO_2 required high temperatures. On the other hand, the cycloaddition of CO_2 and epoxide is an exothermic reaction,[14] which is inhibited at high temperature. Balancing these factors, 413 K was chosen to be the optimal temperature for cycloaddition.

Gas-liquid phase reaction often happens in extreme circumstances since the gas need to dissolve into liquid mixture at a high pressure. In solvent-free synthesis of carbonate, carbon dioxide played a crucial role since it acted as both reactant and solvent. In the pressure range from 0.5 to 2.0 MPa, the ECH conversion and carbonate selectivity both increased with increasing pressure (ESI, Fig. S4B). At low pressures, few CO_2 was dissolved in ECH liquid, limiting the reaction equilibrium. A part of epoxide was hydrolysed to diol side reaction. The diol formed may also then react with carbon dioxide to give the same carbonate product, but the two-step reactions were less efficient than direct cycloaddition. Thus, a low CO_2 pressure will limit the reactivity of both epichlorohydrin and diol, resulting in low ECH conversion and carbonate selectivity. Nevertheless, the reaction carried out at too high CO_2 pressures would cause negative effects. It was once reported that a ring-like intermediate will be produced at high CO_2 pressure.[15] Thus, we choose 2.0 MPa as an optimal pressure for the LMFI-I catalyst in present study.

The reaction time contributed more to the yield of carbonate than to the conversion of epoxide in the cycloaddtion over the LMFI-I catalyst. At 2 h, the ECH conversion already reached 90% with a carbonate yield of 78% (ESI, Fig. S4C). Further prolonging the reaction time to 4 h, the conversion increased little while carbonate yield progressively increased to 85%. This could due to two-step reaction pathways which also produced the carbonate, that is, partial hydrolysis of ECH to diol by the trace amount of water in the system at initial reaction stage and subsequent condensation of diol and CO_2 to carbonate. These reactions happened when diols reached a relatively large amount. Thus, there would be a delay in comparison to direct cycloaddition of epoxide and CO_2. This explains the rise of carbonate yield after three hours of reaction.

The ECH conversion increased progressively with increasing catalyst amount (ESI, Fig. S4D). With a catalyst loading of 25 mg LMFI-I, the ECH conversion was 54%. Increasing the catalyst loading to 100 mg, the ECH reached easily over 90%.

Using organic species as catalytic active sites, their stability are usually concerned. We have investigated the reusability of LMFI-I in cycloaddition reaction (ESI, Fig. S5). The product yield was stable around 90% for the first three times of reuse, indicating a relatively good stability of the catalyst. At the fourth reuse, the ECH conversion dropped slightly to 79%, but the carbonate selectivity remained at 95%. The TEM image indicated that the lamellar structure was well-preserved after reuse (ESI, Fig. S6). The partial deactivation was presumed mainly due to the deposition of heavy byproducts inside zeolite mesopores, blocking the active sites. In particular, the presence of structure directing agent between the zeolite layers may limit the diffusion of product molecules, causing a coke formation.

Based on the results achieved and previously reported literature, a plausible reaction mechanism is proposed for the LMFI-I-catalysed cycloaddition (Scheme1 and ESI, Scheme S1). It is well established that the role of quaternary ammonium halide is to open the three-membered ring of epoxide molecules, giving rise to alkoxide.[16,17] In the reaction system of LMFI-I, the reaction starts with the epoxide molecules approaching to the exposed ammonium cations between layers where the epoxide ring is opened. Iodide attacks at the sterically less hindered β-carbon atom of the epoxide, giving rise to an active oxy anion. The oxy anion then attacks the carbon dioxide, leaving a negative charge on one of the oxygen atom in CO_2. The latter interacts with the carbon atom linked to the oxy anion, allowing iodide to be disconnected, forming a carbonate molecule with a five-member ring structure. The halogen-exchanged organic-inorganic zeolite composite provides the synergistic catalytic active sites that are necessary for the cycloaddition of epoxide and CO_2.

In summary, highly efficient catalysts for the cycloaddition reaction of carbon dioxide to epoxides have been prepared by halogen anion-exchange with the organic-inorganic hybrid zeolites with a lamellar mesostructure. The ammonium cations of SDA and the iodide anions cooperate synergistically for the selective production of carbonates in the absence of solvent and co-catalysts. With a good stability and reusability, this novel material is a promising heterogeneous catalyst for the production of cyclic carbonates in an environmentally friendly way.

The authors gratefully acknowledge the financial supports from the NSFC of China (20973064, 20925310, U1162102), MOST (2012BAE05B02), STCSM (12JC1403600), SMEC (13zz038) and SLAD Project (B409).

Notes and references

Shanghai Key Laboratory of Green Chemistry and Chemical Processes, Department of Chemistry, East China Normal University, North Zhongshan Road 3663, Shanghai 200062, China, Fax: +86-21 62232292; E-mail: pwu@chem.ecnu.edu.cn; hemingyuan@126.com

†Electronic Supplementary Information (ESI) available: details of experimental procedure, material characterizations and catalyst reusability and stability. See DOI:10.1039/b000000x/

1 A. Corma, *J. Catal.*, 2003, **216**, 298.

2 K. Egeblad, C.H. Christensen, M. Kustova and C.H. Christensen, *Chem. Mater.*, 2008, **20**, 946.

3 Y. Tao, H. Kanoh, L. Abrams and K. Kaneko, *Chem. Rev.*, 2006, **106**, 896.

4 a) A. W. Burton, S. Elomari, I. Chan, A. Pradhan and C. Kibby, *J. Phys. Chem. B*, 2005, **109**, 20266.
b) S. Elomari, A. W. Burton, K. Ong, A. R. Pradhan and I. Y. Chan, *Chem. Mater.*, 2007, **19**, 5485.

5 a) J. Sun, C. Bonneau, A. Cantin, A. Corma, M. J. Diaz-Cabanas, M. Moliner, D. Zhang, M. Li and X. Zou, *Nature*, 2009, **458**, 1154.
b) J. Jiang, J. L. Jorda, M. J. Diaz-Cabanas, J. Yu and A. Corma, *Angew. Chem. Int. Ed.*, 2010, **49**, 4986.
c) A. Corma, M. J. Diaz-Cabanas, J. Jiang, M. Afeworki, D. L. Dorset, S. L. Soled and K. G. Strohmaier, *Proc. Natl. Acad. Sci.*, 2010, **107**, 13997.
d) J. Jiang, J. Yu and A. Corma, *Angew. Chem. Int. Ed.*, 2010, **49**, 3120.

6 F. Gramm, C. Baerlocher, L. B. McCusker, S. J. Warrender, P. A. Wright, B. Han, S. B. Hong, Z. Liu, T. Ohsuna and O. Terasaki, *Nature* 2006, **444**, 79.

7 H.G. Karge and J. Weitkamp (Eds.), *Molecular Sieves Science and Technology: Synthesis*, Springer, 1998, 229.

8 G.H. Kuehl and H.K.C. Timken, *Micro. Meso. Mater.*, 2000, **35-36**, 521.

9 H. Lee, S.I. Zones and M.E. Davis, *Micro.Meso.Mater.*, 2006, **88**, 266.

10 Y. Kubota, Y. Nishizaki, H. Ikeya, M. Saeki, T. Hida, S. Kawazu, M. Yoshida, H. Fujii and Y. Sugi, *Micro. Meso. Mater.,* 2004, **70**, 135.

11 M. Choi, K. Na, J. Kim, Y. Sakamoto, O. Terasaki and R.Ryoo, *Nature*, 2009, **461**, 246.

12 L. Xu, C. Li, K. Zhang and P. Wu, *ACS Catal*, 2014, **4**, 2959.

13 J. N. Appaturi and F. Adam, *Appl. Catal. B*, 2013, **136**, 150.

14 C. Guo, X. Zhang, J. Jia and H. Wu, *J. Mol. Struc-Theochem*, 2009, **916**, 125.

15 R. Nomura, M. Kimura, S.Teshima, A. Ninagawa and H. *Matsuda, Bull. Chem. Soc. Jap.*, 1982, **55**, 3200.

16 M. North and R. Pasquale, *Angew. Chem. Int. Ed.*, 2009, **121**, 2990.

17 S. Udayakumar, M. Lee, H. Shim, S. Park, D. Park, *Catal. Comm.*, 2009, **10**, 659.

18 Y. Zhou, S. Hu, X. Ma, S. Liang, T. Jiang and B. Han, *J, Mol. Catal. A*, 2008, **284**, 52.

19 H. S. Kim, J. Y. Bae, J. S. Lee, O. S. Kwon, P. Jelliarko, SD. Lee and S. H. Lee, *J. Catal.*, 2005, **232**, 80.

20 S. Yin and S. Shimada, *Chem Commun,* 2009, **45**, 1136.

21 M. M. Dharman, J. Yu, J. Y. Ahn and D. W. Park, *Green Chem.*, 2009, **11**, 1754.

22 J. W. Huang and M. Shi, *J. Org. Chem.*, 2003, **68**, 6705.

23 J. Sun, L. Wang, S.J. Zhang, Z.X. Li, X.P. Zhang, W.B. Dai and R. Mori, *J. Mol. Catal A*, 2006, **256**, 295.

24 H. Kawanami and Y. Ikushima, *Chem. Commun.*, 2000, **36**, 2089.

25 J.M. Sun, S.I. Fujita, F.Y. Zhao and M. Arai, *Green Chem.*, 2004, **6**, 613.

26 S. S. Wu, X. W. Zhang, W. L. Dai, S. F. Yin, W. S. Li, Y.Q. Ren and C.T. Au, *Appl. Catal* , 2008, **341**, 106.

27 B.M. Bhanage, S.I. Fujita, Y. Ikushima and M. Arai, *Appl. Catal. A,* 2001, **219**, 259.

28 T. Yano, H. Matsui, T. Koike, H. Ishiguro, H. Fujihara, M. Yoshihara, T. Maeshima, *Chem. Commum.*, 1997, **33**, 1129.

29 K. Yamaguchi, K. Ebitani, T. Yoshida, H. Yoshida and K. Kaneda, *J. Am. Chem. Soc.*, 1999, **121**, 4526.